European Journal of Medicinal Chemistry xxx (xxxx) xxx

Contents lists available at ScienceDirect

European Journal of Medicinal Chemistry

journal homepage: http://www.elsevier.com/locate/ejmech

Research paper

A novel class of small molecule inhibitors with radioprotective properties

Jan Marek [a], Ales Tichy [b], Radim Havelek [d], Martina Seifrtova [d], Alzbeta Filipova [b], Lenka Andrejsova [b], Tomas Kucera [c], Lukas Prchal [a], Lubica Muckova [c], Martina Rezacova [d], Zuzana Sinkorova [b], Jaroslav Pejchal [c, *]

[a] Biomedical Research Center, University Hospital Hradec Kralove, Sokolska 581, 500 05, Hradec Kralove, Czech Republic
[b] Department of Radiobiology and Military Pharmacy, Faculty of Military Health Sciences, University of Defence in Brno, Trebesska 1575, 500 01, Hradec Kralove, Czech Republic
[c] Department of Toxicology and Military Pharmacy, Faculty of Military Health Sciences, University of Defence in Brno, Trebesska 1575, 500 01, Hradec Kralove, Czech Republic
[d] Department of Medical Biochemistry, Faculty of Medicine in Hradec Kralove, Charles University, Simkova 870, 500 03, Hradec Kralove, Czech Republic

ARTICLE INFO

Article history:
Received 27 June 2019
Received in revised form
1 August 2019
Accepted 7 August 2019
Available online xxx

Keywords:
1-(2-hydroxyethyl)piperazine derivative
Synthesis
Radioprotection
Ionizing radiation
In vitro
Mice

ABSTRACT

The goal of this study was to develop novel radioprotective agents targeting the intrinsic apoptotic pathway and thus decreasing the radiation-induced damage. For that purpose, we designed, synthesized and analyzed ten new compounds based on the 1-(4-(2-hydroxyethyl)piperazin-1-yl)-3-phenoxypropan-2-ol leading structure. The cytotoxicity of the newly synthesized substances was tested *in vitro* on cell lines derived from different progenitor cells by WST-1 proliferation assay. MTT test was utilized to assess half-maximal inhibitory concentrations and maximum tolerated concentrations of novel compounds in A-549 cells. Screening for radioprotective properties was performed using flow-cytometry in MOLT-4 cells exposed to ^{60}Co ionizing gamma radiation. Selected candidates underwent *in vivo* testing in C57Bl/6 J mice having a positive impact on their immunological status. In summary, we report here promising compounds with radioprotective effect *in vivo*.

1. Introduction

The increasing risk of acute large-scale radiological/nuclear exposures of the population underlines the need to improve efficient radioprotective tools that could be used for radiation protection purposes in public situations such as a nuclear accident, an act of radiologic terrorism, or military conflict [1]. In addition, radiotherapy is still a key modality for treatment of cancer [2]. Unfortunately, it is associated with a number of negative side effects such as the death of bone marrow haematopoietic stem cells or enterocytes, due to the DNA damage, induced signaling pathways, and inflammatory responses and associated generation of reactive oxidative species (ROS), eventually leading to cell death or senescence of cells in normal healthy tissue [3,4].

A radioprotective effect can be achieved through various mechanisms (enhancement of DNA repair, free-radical scavenging, cell synchronization, modulation of growth factors and cytokines, modulation of redox sensitive genes, inhibition of apoptosis, interaction and chelation of the radionuclides, or via gene therapy or stem cell therapy [5]. When searching for an appropriate target, our effort was based on the fact that ionizing radiation (IR) is able to trigger programmed cell death in mammalian cells. While this effect is desirable during radiotherapy of cancer cells, it leads to radiotoxicity in normal healthy tissues.

Two major signaling pathways of apoptosis can be recognized in normal and tumor cells. Extrinsic pathway occurs after ligation of cytokines or factors, such as Tumor necrosis factor alpha (TNF-alpha) or Fas ligand (FasL), to their specific cytoplasmic membrane receptors. In contrast, the intrinsic one is activated by a wide range of stimuli, including growth factor deprivation, oxidants, DNA-damaging agents, or microtubule targeting drugs [6]. We previously identified p53-upregulated mediator of apoptosis (PUMA) as the key molecule of IR-induced cell-death signaling and thus a

* Corresponding author.
E-mail address: jaroslav.pejchal@unob.cz (J. Pejchal).

https://doi.org/10.1016/j.ejmech.2019.111606
0223-5234/

Abbreviations

DMEM	Dulbecco's modified Eagle's medium
DMSO	dimethyl sulfoxide
DOX	doxorubicin
GP	growth percent
HPLC	high performance liquid chromatography
HRMS	high resolution mass spectrometry
i.p.	intraperitoneally
IC_{50}	half maximal inhibitory concentration
IR	ionizing radiation
m. p.	melting point
MS	mass spectrometry
MTC	maximum tolerated concentration
NMR	nuclear magnetic resonance
PBS	phosphate buffer saline
PI	propidium iodide
SEM	standard error of the mean
TLC	thin layer chromatography

promising target in radioprotection, but also in the therapy of neurodegenerative and cardiovascular diseases [7]. PUMA is often associated with IR-induced apoptosis and it can be upregulated in both p53-dependent and p53-independent manner [8–12].

In this paper, we present the basic characteristics of novel compounds - derivatives of 1-(4-(2-hydroxyethyl)piperazin-1-yl)-3-phenoxypropan-2-ol that was screened and selected as one of the leading structures by Mustata et al., in 2011 [13]. Cytotoxicity screening was performed on a panel of human cell lines. *In vitro* experiments were carried out in order to assess basic parameters such as half-maximal inhibitory concentration (IC_{50}), maximum tolerated concentration (MTC), and inhibition of IR-induced apoptosis in selected cell lines. Finally, the most promising compounds were subjected to *in vivo* tests on whole-body irradiated mice in order to evaluate their radioprotective potential.

2. Results and discussion

2.1. Compounds

Several published structures are already mentioned in the literature. The patent ES411826 describes the preparation of compounds 3b, 3c, 3f, 3j, and 3i without specification of the preparation process or usage [14]. Some compounds (3a, 3b, 3c, 3 g, and 3 h) are mentioned in ZINC database, again without the preparation process and biological activities [15–18]. A similar strategy of preparation process of aryloxy derivatives (preparation of **2a-j**) was found in the literature [19–22]. These compounds were published as antiviral agents, adrenoceptor antagonists or platelet aggregation inhibitors. Compounds 3b and 3c had already been published by Mustata et al., in 2011 as PUMA inhibitors [13]. Nevertheless, the preparation process and *in vivo* activity are not mentioned here. The **3e** analogue was not found elsewhere.

2.2. In silico study

The selected compounds underwent a docking study with anti-apoptotic Bcl-2 protein involving its interaction site with pro-apoptotic PUMA, which negatively regulates Bcl-2 protein and triggers apoptosis [23].

An example is illustrated in Fig. 1, depicting the docking pose of the ligand **3e**. It shows hydrogen bond interactions of the hydroxyl group with Asp108 and Arg143, of the methoxy-group with Arg143, of the ether oxygen with Arg143, of the distal hydroxymethyl group with Arg126, and of the protonated nitrogen with Met112. The docking pose was compared with the pose of a bavitoclax analog co-crystallized with Bcl-2. Both of them have an aromatic ring placed in the lipophilic cavity bordered by Phe101 and Phe109. Surprisingly, the piperazine motif of **3e** is located differently from the bavitoclax analog. Therefore, the protonated nitrogen of piperazine can interact with Glu133.

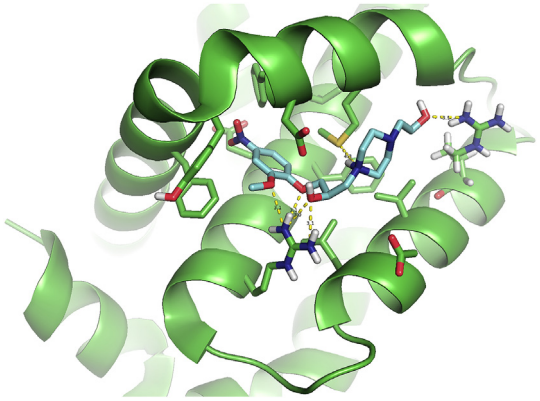

Fig. 1. Docking pose of the ligand 3e in the cavity of Bcl-2 protein.

The docking study indicates that our compounds might interfere with anti-apoptotic and pro-apoptotic protein interaction with possible implications for cell-death signaling.

2.3. Synthesis and analysis

The general synthetic procedure for the novel 1-(4-(2-hydroxyethyl)piperazin-1-yl)-3-phenoxypropan-2-ol like compounds is displayed in Scheme 1. The first step is reaction of the appropriate aryl alcohol (**1a-j**) with an excess of epibromohydrin under reflux for 2 h in the presence of piperazine (i), according to the process published by Kreighbaum et al. [20]. These solvent-free reactions led to the preparation of intermediates **2a-j**. Purification by column chromatography gave yields of around 80%. The purity of intermediates **2a-j** was relatively low (around 60–70%), but sufficient for the second step of the reaction. The next step involved the alkylation of 1-(2-hydroxyethyl)piperazine by the differently-substituted intermediates **2a-j**, resulting in compounds **3a-j**. The reactions were refluxed with potassium carbonate in acetonitrile for 4 h (ii). The crude products were purified by column chromatography, with yields ranging from 57 to 81% (Table 1) and sufficient purity (≥95%). Finally, the compounds (**3a-j**) were converted into their more soluble hydrogen chloride salts by treatment with hydrochloric acid in methanol. All of the 1-(4-(2-hydroxyethyl) piperazin-1-yl)-3-phenoxypropan-2-ol derivatives were additionally characterized by the ^{1}H and ^{13}C nuclear magnetic resonance (NMR) spectra and high resolution mass spectrometry (HRMS). All analytical measurements confirmed the structure and high purity of the prepared compounds. The detailed analyses of all compounds are provided in the Supporting information.

2.4. In vitro cytotoxicity

The cytotoxicity of the 10 new inhibitors at concentrations of 10 and 100 μM was determined on a screening panel of 10 human cell lines, including 9 human cancerous cell lines and 1 non-cancerous cell line. Doxorubicin at a concentration of 1 μM was used as a positive control. The cell lines were exposed to these compounds

Please cite this article as: J. Marek et al., A novel class of small molecule inhibitors with radioprotective properties, European Journal of Medicinal Chemistry, https://doi.org/10.1016/j.ejmech.2019.111606

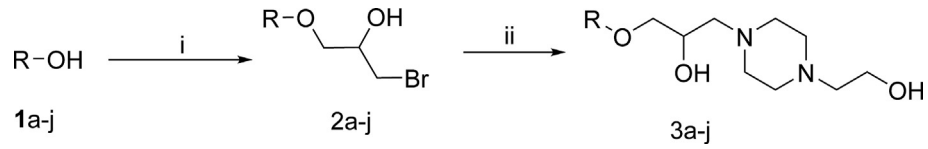

Scheme 1. Synthetic pathway of 1-(4-(2-hydroxyethyl)piperazin-1-yl)-3-phenoxypropan-2-ol like derivatives (**3a-j**). Reagents and conditions: (i) Epibromohydrin, 135 °C, 2 h, 1 drop of piperazine; (ii) 1-(2-hydroxyethyl)piperazine, acetonitrile, reflux, 4 h.

Table 1
Structures, yields and C log P of prepared compounds.

Compound	R	Yield (%)	C log P
3a	1-naphthyl	65	1,35
3b	2-naphthyl	57	1,35
3c	4-methyl-1-phenyl	74	0,874
3d	Phenyl	77	0,361
3e	4-nitro-2-methoxy-1-phenyl	81	0,143
3f	2-isopropyl-5-methyl-1-phenyl	72	2119
3g	2,6-dimethoxy-1-phenyl	59	0,046
3h	4-allyl-2-methoxy-1-phenyl	64	1302
3i	2-methoxy-1-phenyl	71	0,203
3j	2-methyl-1-phenyl	75	0,874

for 48 h. Cell proliferation was then determined by WST-1 proliferation assay and related to the proliferation of untreated control cells (100%). The results have shown that the inhibitors had no cytotoxic effect at 10 μM in all 10 cell lines, the percentage of viable cells varying from 87% to 112%. At a concentration of 100 μM, compound **3a** decreased the viability of HT-29 and MCF-7 cells to 53% and 64%, respectively. Similarly, compounds **3f** and **3h** showed a mild cytotoxic effect in HT-29 and MOLT-4 with the percentage of viable cells being 64% and 65%, respectively. The other compounds showed no signs of cytotoxicity at 100 μM. The data of all screened compounds for each cell line are presented in Tables 2a and 2b.

To express the overall inhibitory activity of each compound, the growth percent value (GP) was calculated. GP represents the mean viability of 10 cell lines treated with the same concentration. The compounds at 10 μM concentrations showed no cytotoxic effect. At this concentration, GP values were 96%–103%. At the higher 100 μM concentration, the GP values ranged from 86% to 102% (Fig. 2). The basic screening at a given concentration showed no significant cytotoxic effect in any tested compound.

2.5. Half maximal inhibitory concentration (IC_{50}) and maximum tolerated concentration (MTC)

In addition to WST-1 proliferation assay, MTT test was carried out to provide information on toxicological indexes of the new compounds, including IC_{50} and MTC. MTT assay is a sensitive colorimetric method assessing metabolic activity of cells. The method is suitable for adherent cell lines. Therefore, A-549 cell line was randomly selected for the test.

In A549 cells, the lowest toxicity was detected in compound **3i** ($IC_{50} = 9.27 \pm 1.18$ mM) using MTT assay. The toxicity of potential radioprotective compounds increased from **3i** towards **3g**, **3d**, **3e**, **3j**, **3c**, **3h**, **3a**, **3f**, and **3b** with IC_{50} values being 1.2-, 1.6-, 2.1-, 2.7-, 3.8-, 8.3-, 22.1-, 25.8-, and 29.9 lower than in **3i** treated cells (Table 3). In relation to the structure, it is evident that the tolerability of cells is lower for compounds with larger substituents (**3a**, **3b**) or additional alkyl substituents on the phenyl ring (**3f**). The data indicates that increased lipophilicity is associated with cytotoxicity [24]. The correlation of ClogP value with toxicity status of the prepared compounds is obvious.

2.6. Protective effect on irradiated cell lines

The radioprotective effect of the ten compounds was evaluated by flow cytometric detection of Annexin V/propidium iodide positive cells. To avoid interference of the detachment procedure with the binding of Annexin V to the cytoplasmic membrane, non-adherent MOLT-4 lymphoblastic leukemia cells were selected for the testing.

Novel potential radioprotectives improved the viability of MOLT-4 cells *in vitro*. As per Fig. 3A, the Annexin V/propidium iodide (PI) staining clearly demonstrates the decline in the percentage of viable cells 24 h after gamma irradiation by a dose of 1 Gy

Table 2a
Cytotoxic effect of inhibitors on 10 human cell lines. Values represent cell viability after treatment with the compounds at doses of 10 μM. The results are expressed as percentage of viability of untreated control cells (100%). DOX – doxorubicin (1 μM). Each value is a mean of three independent experiments ± SD. Values from the intervals 0–25%, 26–50% and 50–75% are highlighted with different colors.

	3a	3b	3c	3d	3e	3f	3g	3h	3i	3j	DOX
Jurkat	96 ± 7	97 ± 2	101 ± 11	104 ± 2	101 ± 6	97 ± 3	110 ± 9	110 ± 6	106 ± 5	106 ± 5	2 ± 0
MOLT-4	98 ± 1	109 ± 2	103 ± 5	92 ± 10	92 ± 7	87 ± 5	105 ± 5	104 ± 6	100 ± 12	104 ± 6	1 ± 0
A549	98 ± 12	102 ± 1	106 ± 12	97 ± 9	93 ± 8	90 ± 17	97 ± 8	91 ± 9	91 ± 4	95 ± 7	42 ± 11
HT-29	93 ± 5	92 ± 2	98 ± 3	97 ± 3	99 ± 2	93 ± 3	102 ± 6	109 ± 8	93 ± 6	98 ± 2	55 ± 18
PANC-1	102 ± 4	101 ± 3	102 ± 8	90 ± 9	92 ± 13	91 ± 12	104 ± 5	101 ± 7	100 ± 9	102 ± 4	78 ± 7
A2780	97 ± 4	99 ± 1	97 ± 9	96 ± 4	99 ± 4	100 ± 3	95 ± 8	97 ± 11	100 ± 4	101 ± 4	8 ± 4
HeLa	99 ± 9	109 ± 4	100 ± 3	95 ± 5	101 ± 4	105 ± 8	101 ± 14	100 ± 21	93 ± 10	102 ± 4	76 ± 12
MCF-7	103 ± 5	93 ± 5	107 ± 3	104 ± 4	103 ± 5	100 ± 4	101 ± 7	99 ± 8	99 ± 3	103 ± 6	32 ± 3
SAOS-2	97 ± 7	98 ± 4	102 ± 11	102 ± 7	103 ± 8	93 ± 10	106 ± 3	112 ± 5	106 ± 6	103 ± 10	22 ± 4
MRC-5	102 ± 9	103 ± 2	112 ± 13	101 ± 4	97 ± 4	102 ± 9	973 ± 17	94 ± 14	90 ± 10	97 ± 12	22 ± 2

Please cite this article as: J. Marek et al., A novel class of small molecule inhibitors with radioprotective properties, European Journal of Medicinal Chemistry, https://doi.org/10.1016/j.ejmech.2019.111606

Table 2b
Cytotoxic effect of inhibitors on 10 human cell lines. Values represent cell viability after treatment with the compounds at doses of 100 μM. The results are expressed as percentage of viability of untreated control cells (100%). DOX – doxorubicin (1 μM). Each value is a mean of three independent experiments ± SD. Values from the intervals 0–25%, 26–50% and 50–75% are highlighted with different colors.

	3a	3b	3c	3d	3e	3f	3g	3h	3i	3j	DOX
Jurkat	76 ± 4	96 ± 2	97 ± 1	91 ± 4	92 ± 5	98 ± 6	84 ± 11	83 ± 12	86 ± 11	92 ± 11	2 ± 0
MOLT-4	83 ± 5	100 ± 4	103 ± 2	96 ± 2	99 ± 8	90 ± 4	76 ± 5	65 ± 7	76 ± 4	86 ± 8	1 ± 0
A549	107 ± 12	102 ± 18	110 ± 26	99 ± 0	105 ± 2	114 ± 3	99 ± 9	105 ± 7	109 ± 25	114 ± 10	42 ± 11
HT-29	53 ± 2	103 ± 3	107 ± 19	97 ± 1	111 ± 15	64 ± 6	141 ± 10	102 ± 9	143 ± 4	151 ± 6	55 ± 18
PANC-1	101 ± 2	95 ± 2	99 ± 2	108 ± 9	105 ± 11	125 ± 9	115 ± 3	116 ± 3	115 ± 11	116 ± 7	78 ± 7
A2780	77 ± 1	91 ± 2	94 ± 2	96 ± 2	95 ± 4	90 ± 7	83 ± 3	85 ± 5	78 ± 4	79 ± 8	8 ± 4
HeLa	129 ± 0	116 ± 7	101 ± 12	107 ± 5	108 ± 2	132 ± 7	94 ± 6	99 ± 13	99 ± 8	96 ± 11	76 ± 12
MCF-7	64 ± 2	93 ± 4	100 ± 7	98 ± 2	98 ± 5	85 ± 4	90 ± 6	89 ± 8	95 ± 7	95 ± 9	32 ± 3
SAOS-2	97 ± 2	91 ± 0	83 ± 2	96 ± 3	94 ± 3	109 ± 3	82 ± 4	75 ± 4	82 ± 12	84 ± 8	22 ± 4
MRC-5	78 ± 3	98 ± 7	100 ± 4	101 ± 9	97 ± 5	90 ± 6	115 ± 10	103 ± 9	109 ± 17	104 ± 25	22 ± 2

stand-alone (40%) as compared to the untreated cells (92%). Conversely, pretreatment with compounds **3a-3j** at 100 μM 1 h before gamma irradiation exerted protective effects against ionizing radiation-induced death of MOLT-4 cells. In the 24 h interval after the exposure to IR, the amount of viable cells increased up to 65%, 59%, 52%, and 62% after being pretreated with inhibitors **3b**, **3e**, **3h**, and **3j**, respectively, when compared to only IR-treated cells (Fig. 3B).

2.7. Radioprotective effect on mice

Compounds for this stage of study were selected based on toxicological evaluation and physico-chemical properties. Compounds **3b**, **3e**, **3h**, and **3j** significantly improved the viability of irradiated MOLT-4 cells *in vitro*; however, compound **3b** induced undesired effects when applied to healthy mice and possessed the lowest solubility. Thus, it was excluded from further testing. Compounds **3g** and **3i** showed the lowest toxicity/highest MTC when applied to A549 cells and were therefore included in the *in vivo* radioprotective study.

2.7.1. Safety of selected compounds in vivo

The experimental mice were injected (i.p.) with 100 mg/kg of tested substances **3e**, **3g**, **3h**, **3i**, and **3j**.

The selected compound administered at this dose appeared to be safe, with no deaths or adverse effects recorded within the 30-day interval. Weight gain was similar to the control group (Table 4).

2.7.2. Treatment with potential radioprotectives prolongs mice survival after gamma irradiation

To assess radioprotective properties of selected substances, the animals were injected (i.p.) with 100 mg/kg of **3e**, **3g**, **3h**, **3i**, and **3j** 5 min before receiving an IR dose of 8.5 Gy. This dose can be considered as supra-lethal for the C57BL/6 J mouse strain with LD_{50} ranging from 7.76 to 8.05 Gy [25–27]. The radioprotection effect of these compounds was assessed for 30 days after irradiation.

Survival curves are presented in Fig. 4, median survival values are summarized in Table 5, and weight gain of surviving animals is shown in Table 6. The substances did not affect animal survival with one exception. Substance **3j** significantly decreased mouse survival from 12 to 7 days. The mechanism underlying this effect remains unknown. We may only hypothesize that **3j** interacts with Bcl-2 or possibly other anti-apoptotic Bcl-2 members and inhibits its anti-apoptotic action. If confirmed, such substance could be of potential value as an anticancer agent [28]. Other tested substances, including 3e, 3 g, 3 h, and 3i, increased survival from 0% to 40%, 20%, 30%, and 30%, respectively; however, this increase was not statistically significant.

2.7.3. Impact of the compounds on the immunological status of irradiated mice

Fig. 5 shows that the i.p. application of compound **3j** significantly decreased the absolute number of lymphocytes in non-irradiated animals (0 Gy) 7 and 12 days after the treatment, whereas substance **3h** showed a similar effect in the 12 day interval. Fig. 6 demonstrates that the immunotoxicity of **3j** was directed selectively towards B-lymphocytes.

In contrast, a significantly increased trend in the absolute number of lymphocytes in irradiated mice was observed in groups treated with the compounds **3e** (day 12, day 30) and **3i** (day 30; Fig. 5). Substance **3e** showed the most pronounced radioprotective effect, maintaining a significant B cell population throughout the experiment and supporting T and NK cell populations in the later time intervals (Fig. 6).

3. Conclusion

Despite the current large-scale screening of thousands of synthetic or natural compounds with the goal of finding an appropriate radioprotective agent, only a few of them find application in clinical practice. As an example, antioxidants scavenging ROS, such as amifostine, alpha-tocopherol (vitamin E), curcumin, or metformin, have shown very promising results [29,30]. Other agents, including angiotensin converting enzyme inhibitors, statins or immunosuppressive agents, have been demonstrated to target inflammatory pathways [29]. However, there is a concern that such therapies, given concomitantly with radiotherapy, could reduce tumor control rates.

With a deeper molecular understanding of pathways involved in response to ionizing radiation, new targeted therapies could be developed with the advantage of greater specificity towards diverse molecular pathways activated in various distinct cell types (e.g. tumor vs. nonmalignant). Multitude of pathways is involved in cell death following irradiation – apoptosis induction by intrinsic

Please cite this article as: J. Marek et al., A novel class of small molecule inhibitors with radioprotective properties, European Journal of Medicinal Chemistry, https://doi.org/10.1016/j.ejmech.2019.111606

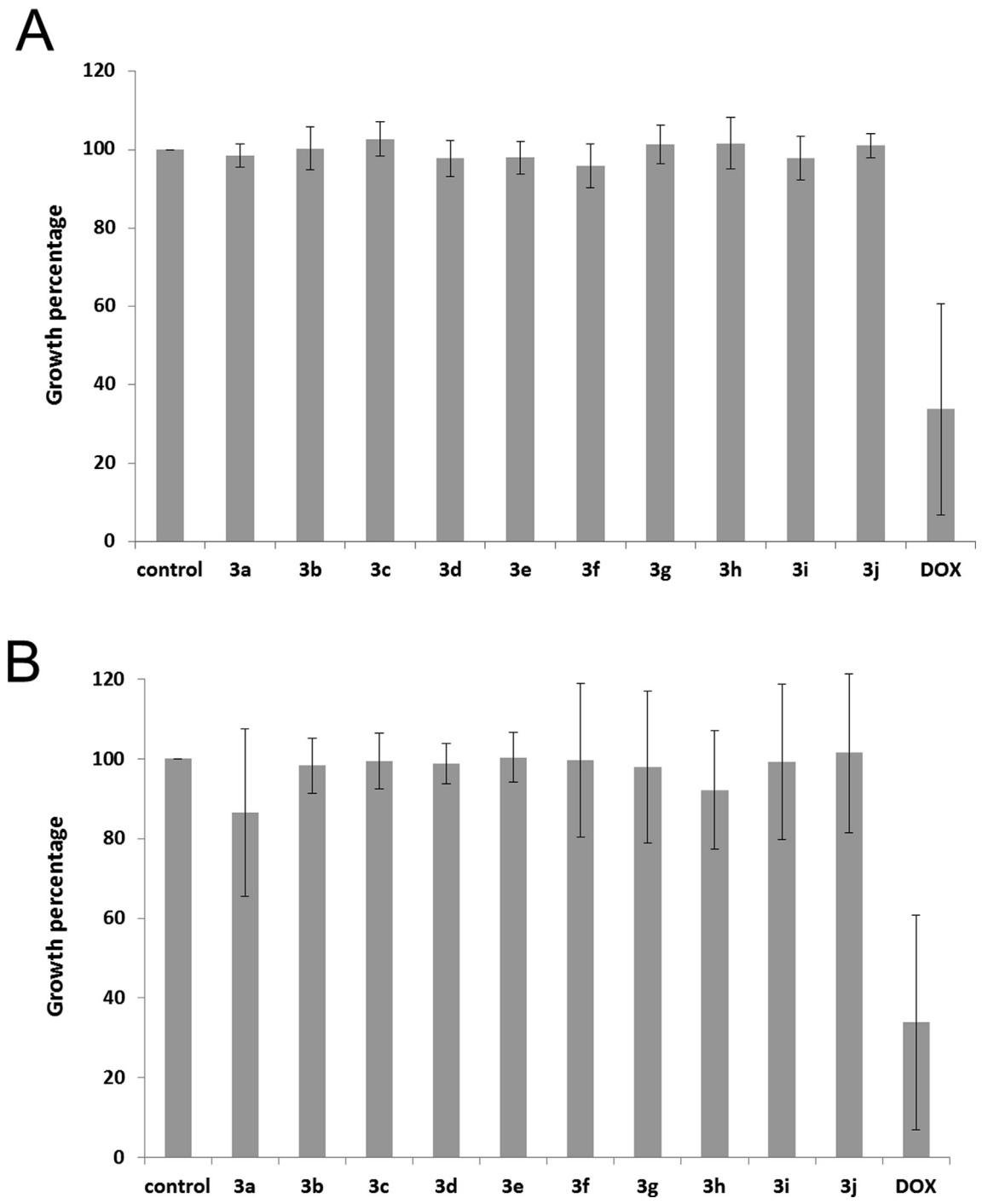

Fig. 2. Viability of tested cell lines Growth percent value was calculated for each compound at 10 μM (A) and 100 μM (B) concentration. The values represent the average viability (expressed as percent of control) of all the 10 cell lines. Control: untreated cells, DOX – doxorubicin (1 μM).

pathway, but also chronic inflammation and oxidative stress [31,32], as well as DNA repair suppression. All of these could be a target of possible radioprotective small molecular inhibitors. Our efforts were driven by the hypothesis that small molecule inhibitors targeting the apoptosis pathway (particularly those interfering with Bcl-2 proteins interaction) should exhibit radioprotective properties. Supported by initial docking study data, we designed a group of potentially radioprotective compounds. These might be applied as inhibitors of pro-apoptotic and anti-apoptotic protein-protein interactions with obvious impact on radiation-induced cell death signaling. This might have great implications not only for radioprotection but also for other areas such as the therapy of neurodegenerative and cardiovascular diseases that rely on the apoptotic pathway [7].

For this study, our team built a unique pipeline consisting of *in silico* study, in-house synthesis, physicochemical analysis, *in vitro* cytotoxicity and *in vivo* toxicity testing followed by radioprotective effect evaluation. As an outcome of this approach we report the synthesis and biological characterization of a novel series of 1-(4-(2-hydroxyethyl)piperazin-1-yl)-3-phenoxypropan-2-ol

Please cite this article as: J. Marek et al., A novel class of small molecule inhibitors with radioprotective properties, European Journal of Medicinal Chemistry, https://doi.org/10.1016/j.ejmech.2019.111606

Table 3
Toxicity of new inhibitors in A549 cells measured using MTT assay.

Compounds	$IC_{50} \pm SEM$ (mM)	MTC (mM)
3a	0.42 ± 0.04	0.07
3b	0.31 ± 0.02	0.02
3c	2.43 ± 0.16	0.29
3d	5.78 ± 0.30	0.59
3e	4.45 ± 0.05	0.78
3f	0.36 ± 0.01	0.16
3g	7.81 ± 0.48	1.56
3h	1.12 ± 0.10	0.20
3i	9.27 ± 0.68	1.56
3j	3.40 ± 0.05	0.39

MTC: maximum tolerated concentration, i.e. the highest concentration showing no significant difference in comparison with non-treated control (*t*-test).

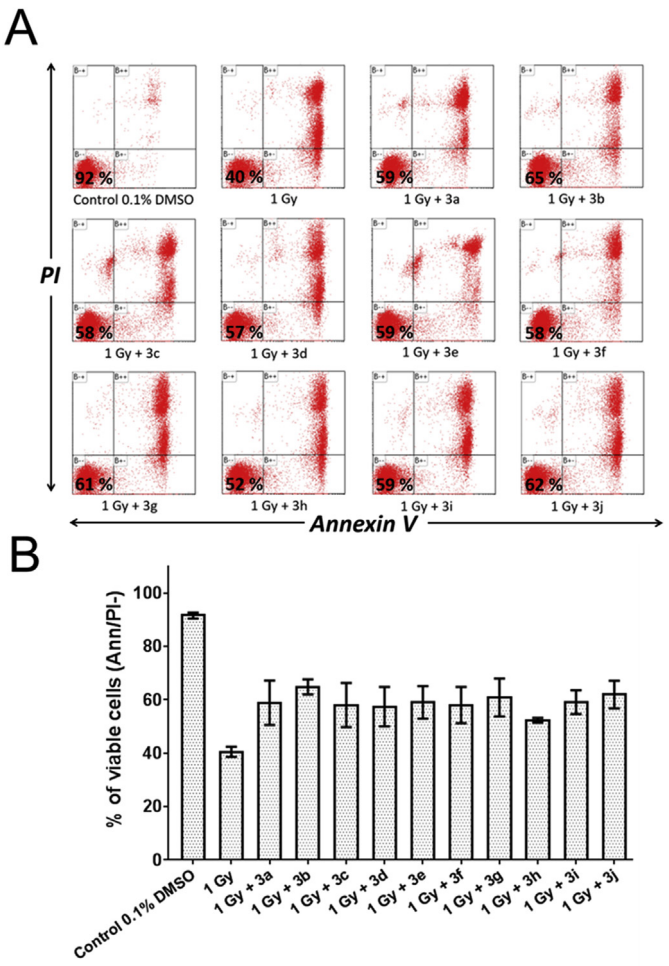

Fig. 3. The viability of MOLT-4 cells after the exposure of ionizing radiation stand-alone or in combination with novel compounds at 100 μM concentration Viability of MOLT-4 cells was determined as the percentage of Annexin-V and propidium iodide (PI)-double-negative cells by flow cytometry 24 h following irradiation by a dose of 1 Gy. (A) Representative flow cytometry histograms depicting the percentage of viable MOLT-4 cells are shown. (B) The bar graph represents the percentage of viable MOLT-4 cells detected by flow cytometry as Annexin V negative/PI negative cells. Results are shown as the mean ± SD from four experiments.

derivatives as compounds with radioprotective properties.

We modified the aryl moiety of our leading structure to prepare an entire group of compounds. The influence of substituents has been compared with the important parameter of solubility, which is often limiting for further biological tests. We managed to prepare

Table 4
Average weight of mice before (day 0) and after (day 30) the treatment with selected compounds (100 mg/kg) ± SD.

	Control (g)	3e (g)	3 g (g)	3 h (g)	3i (g)	3j (g)
Day 0	26.3 ± 2.4	27.8 ± 2.3	27.0 ± 0.9	25.7 ± 2.5	27.9 ± 4.4	26.2 ± 2.0
Day 30	27.0 ± 3.2	28.5 ± 2.9	27.6 ± 2.1	27.0 ± 2.3	28.5 ± 4.6	27.2 ± 2.7
%	103 ± 12	103 ± 10	102 ± 8	105 ± 9	102 ± 16	104 ± 10

%: procentage change since day 0 (100%).

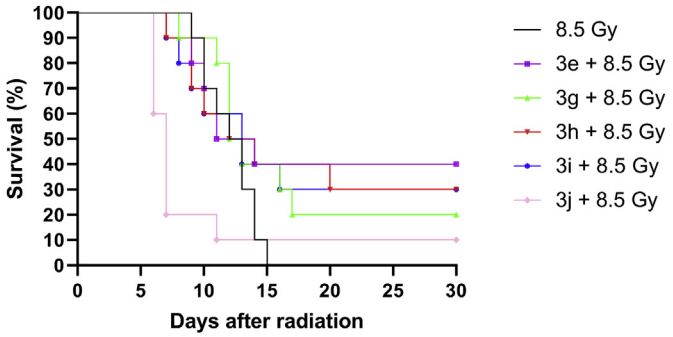

Fig. 4. Survival curves of irradiated mice and irradiated mice injected (i.p.) with selected compounds **3e**, **3g**, **3h**, **3i**, and **3j** for 30 days.

Table 5
Median survival values of irradiated mice treated (i.p.) with selected compounds **3e**, **3g**, **3h**, **3i**, and **3j** for 30 days.

Group	Median survival in days (95% confidence interval)
saline + 8.5 Gy	12 (9.9–14.1)
3e + 8.5 Gy	11 (6.9–15.1)
3 g + 8.5 Gy	12 (10.5–13.6)
3 h + 8.5 Gy	12 (5.8–18.2)
3i + 8.5 Gy	13 (8.4–17.6)
3j + 8.5 Gy	7 (6.4–7.6)[a]

[a] $p \leq 0.05$ when compared with saline-treated mice.

Table 6
Average weight of mice before (day 0) and after (day 30) the treatment with selected compounds (100 mg/kg) and combined with gamma radiation (8.5 Gy) ± SD.

	Control (g)	3e (g)	3 g (g)	3 h (g)	3i (g)	3j (g)
Day 0	25.4 ± 2.6	26.1 ± 1.9	27.3 ± 1.6	25.1 ± 2.5	26.8 ± 2.1	27.3 ± 1.4
Day 30	†	26.5 ± 2.4	27.7 ± 0.9	27.3 ± 1.2	27.6 ± 1.9	‡
%	†	101 ± 3	109 ± 5	103 ± 7	102 ± 9	‡

%: procentual change since day 0 (100%).
† Mice lost (death) before the analysis could be performed.
‡ Analysis was not performed – only one mouse left.

well-soluble substances. Beyond that, the presented data show that our compounds had no cytotoxic effect on 10 human cell lines (even at 100 μM). Subsequently, we measured the maximum tolerable concentration for all compounds.

Furthermore, we evaluated the protective effect on irradiated MOLT4 cells. Finally, we selected the most suitable compounds based on their toxicological and physicochemical profile. We have performed *in vivo* study on whole-body irradiated mice. Importantly, we observed an interesting structural relationship between the methoxy group in position 2 on the aromatic ring and an improved radioprotective effect of our compounds. That said, analogue **3e** was determined as the most effective radioprotective compound. The data from *in vitro* experiments related to radioprotection were comparable with other compounds, but the *in vivo* radioprotective effect together with MTC indicate that analogue **3e**

Please cite this article as: J. Marek et al., A novel class of small molecule inhibitors with radioprotective properties, European Journal of Medicinal Chemistry, https://doi.org/10.1016/j.ejmech.2019.111606

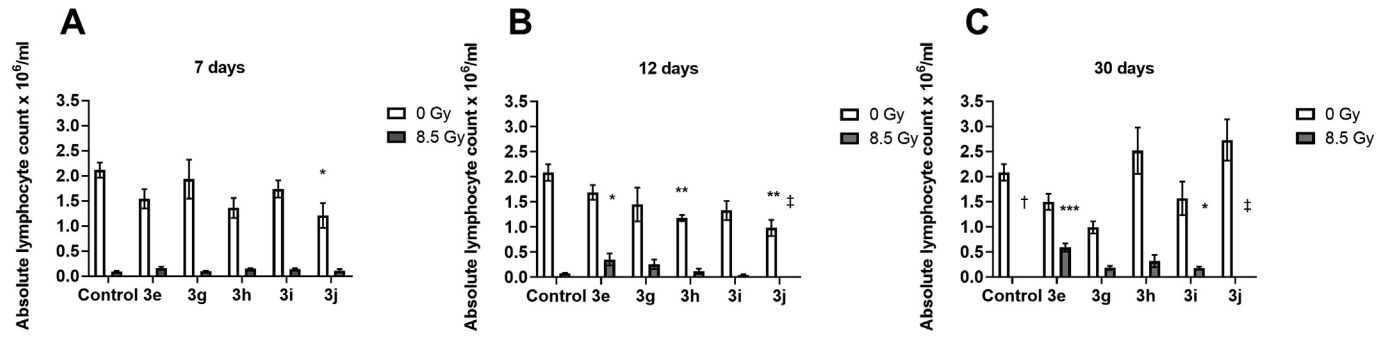

Fig. 5. Absolute lymphocyte counts in peripheral blood after the application of **3e**, **3g**, **3h**, **3i**, and **3j** (100 mg/kg) in non-irradiated and radiated mice at (A) 7, (B) 12 and (C) 30 days post-treatment. Inhibitors were applied i.p. 5 min before irradiation by a single dose of 8.5 Gy. Values represent the mean ± SEM. *p < 0.05, **p < 0.01, ***p < 0.001. † Mice lost (death) before the analysis could be performed. ‡ Analysis was not performed – only one mouse left.

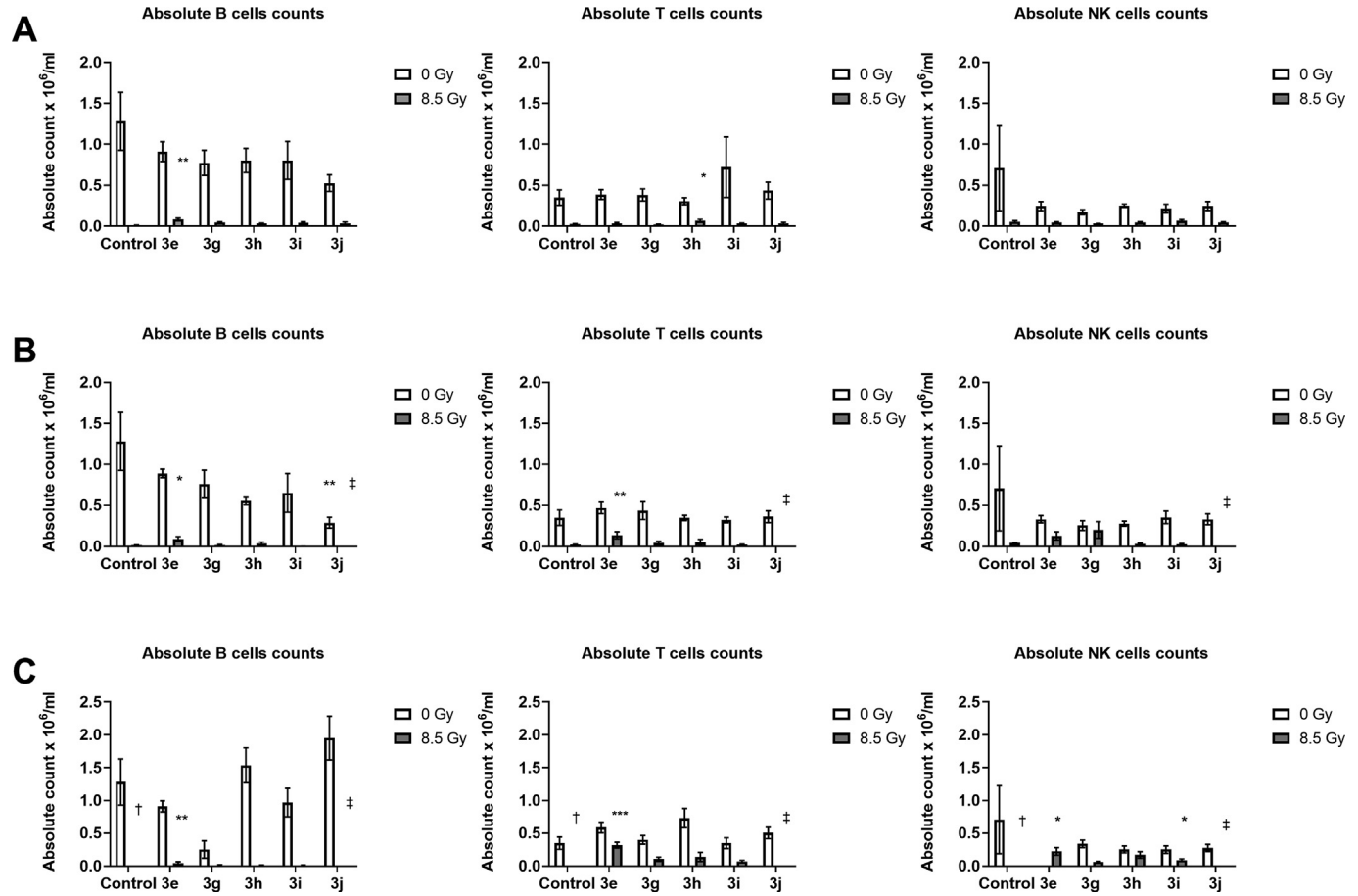

Fig. 6. Effect of radioprotectives (**3e**, **3g**, **3h**, **3i**, and **3j**; 100 mg/kg) on the proportion of B- and T-lymphocytes and NK cells in non-irradiated and irradiated mice at (A) 7, (B) 12, and (C) 30 days post-radiation. Inhibitors were applied i.p. 5 min before irradiation by a single dose of 8.5 Gy. Values represent the mean ± SEM. *p < 0.05, **p < 0.01, ***p < 0.001. † Mice lost (death) before the analysis could be performed. ‡ Analysis was not performed – only one mouse left.

possesses the highest potential as the radioprotective therapeutic utility.

Further research is ongoing in order to reveal a mechanistic explanation of the radioprotective effect, but as our *in silico* data indicate, the compounds are likely to interfere with Bcl-2 protein-protein interaction, interfering with apoptosis induction. The actual mechanistic explanation will be necessary to design patient-tailored radioprotection in cancers with dysfunctional intrinsic apoptotic pathways. It should be also noted that in radiosensitive organs (such as bone marrow) immune system activation and signaling mechanism (involving FasL, TNF-alpha, nitric oxide, and superoxide) contribute to cell death [33]. Synergic combination of small molecule inhibitor targeting intrinsic apoptotic pathway together with an anti-inflammatory drug could be an effective strategy for radioprotection in mass casualty scenarios.

4. Experimental

4.1. In silico study

The 3D structure of Bcl-2 was gained from RCSB Protein Data Bank – PDB ID 4LXD (Bcl_2-Navitoclax Analog complex) [23]. The

Please cite this article as: J. Marek et al., A novel class of small molecule inhibitors with radioprotective properties, European Journal of Medicinal Chemistry, https://doi.org/10.1016/j.ejmech.2019.111606

structure was inspected and found as suitable for molecular docking – it's resolution is 1,9 Å and it has no outliers according to Ramachandran's plot [34] The receptor structure was prepared by the DockPrep function of UCSF Chimera (version 1.4) [35] and converted to pdbqt-files by AutodockTools (v. 1.5.6) [36]. Three-dimensional structures of ligands were built by Open Babel (v. 2.3.1) [37], minimized by Avogadro (v 1.1.0) [38], and converted to pdbqt-file format by AutodockTools [36]. The docking calculations were done by Autodock Vina (v 1.1.2) with an exhaustiveness of 8 [39]. Calculation was done 15 times for each ligand and receptor, and the best-scored result was selected for manual inspection. The visualization of enzyme–ligand interactions was prepared using Pymol (v. 1.7.4.5) [The PyMOL Molecular Graphics System, Version 1.7.4.5, Schrödinger, LLC, Mannheim, Germany].

4.2. Synthesis and analysis

Analytical grade reagents were purchased from Sigma-Aldrich, Fluka and Merck (Darmstadt, Germany). The solvents were purchased from Penta Chemicals (Prague, Czech Republic). Reactions were monitored by thin layer chromatography (TLC) using precoated silica gel 60 F_{254} TLC aluminium sheet. Column chromatography was performed with silica gel 0.063–0.200 mm. Melting points (m. p.) were determined on a microheating stage PHMK 05 (VEB Kombinat Nagema, Radebeul, Germany) and are uncorrected. All compounds were fully characterized by NMR spectra and HRMS. NMR spectra were recorded on Varian VNMR S500 (operating at 500 MHz for H^1 and 125 MHz for C^{13}; Varian Comp., Palo Alto, USA). The chemical shifts (δ) are given in ppm, related to tetramethylsilane (TMS) as internal standard. Coupling constants (J) are reported in Hz. Splitting patterns are designated as s, singlet; d, doublet; t, triplet; dd, doublet of doublets; and m, multiplet. Mass spectra were recorded using a combination of liquid chromatography and mass spectrometry: high resolution mass spectra (HRMS) and sample purities were obtained by high performance liquid chromatography (HPLC) with UV and mass spectrometry (MS) gradient method. The system used in this study was Dionex Ultimate 3000 UHPLC: RS Pump, RS Column Compartment, RS Autosampler, Diode Array Detector, Chromeleon (version 6.80 SR13 build 3967) software (Thermo Fisher Scientific, Germering, Germany) with Q Exactive Plus Orbitrap mass spectrometer with Thermo Xcalibur (version 3.1.66.10.) software (Thermo Fisher Scientific, Bremen, Germany). Detection was performed by mass spectrometry in positive mode. Settings of the heated electrospray source were: Spray voltage 3.5 kV, Capillary temperature: 220 °C, Sheath gas: 55 arbitrary units, Auxiliary gas: 15 arbitrary units, Spare gas: 3 arbitrary units, Probe heater temperature: 220 °C, Max spray current: 100 μA, S-lens RF Level: 50. C18 column (Kinetex EVO C18, 3 × 150 mm, 2.6 μm, Phenomenex, Japan) was used in this study. Mobile phase A was ultrapure water of ASTM I type (resistance 18.2 MΩ cm at 25 °C) prepared by Barnstead Smart2Pure 3 UV/UF apparatus (Thermo Fisher Scientific, Bremen, Germany) with 0.1% (v/v) formic acid (LC-MS grade, Sigma Aldrich, Steinheim, Germany); mobile phase B was acetonitrile (MS grade, Honeywell-Sigma Aldrich, Steinheim, Germany) with 0.1% (v/v) of formic acid. The flow was constant at 0.4 ml/min. The method started with 1 min of isocratic flow of 10% B, and then the gradient of B rose to 100% B in 3 min and remained constant at 100% B for 1 min. The composition then went back to 10% B and equilibrated for 2.5 min. Samples were dissolved in methanol (LC-MS grade, Fluka-Sigma Aldrich, Steinheim, Germany) at concentration 1 mg/ml and sample injection was 1 μl. Purity was determined from UV spectra measured at wavelength 254 nm. HRMS was determined by total ion current spectra from the mass spectrometer.

Clog P was calculated with MarvinSketch (version 14.9.8.0) software.

4.2.1. General procedure for synthesis of 1-(4-(2-hydroxyethyl) piperazin-1-yl)-3-phenoxypropan-2-ol derivatives (**3a**-**3j**)

1-(2-hydroxyethyl)piperazine (0.2 g, 1.5 mmol) was dissolved in anhydrous acetonitrile and K_2CO_3 (0.4 g, 3.0 mmol) with appropriate intermediate (**2a**-**2j**) were added. The reaction mixture was stirred under a nitrogen atmosphere for 4 h. The mixture was filtered and the filtrate concentrated under reduced pressure. The residue was purified by flash chromatography eluting with EtOAc/MeOH/NH_3 (25% aq) (6:2:0.2) to obtain yellow or white product in 57–81% yields.

*4.2.1.1. 1-(4-(2-hydroxyethyl)piperazin-1-yl)-3-(naphthalen-1-yloxy)propan-2-ol (**3a**).* Yellow oil (0,43 g, 86%); ^{1}H NMR (500 MHz, Methanol-d_4) δ 8.31 (dd, J = 7.6, 1.9 Hz, 1H), 7.83–7.75 (m, 1H), 7.51–7.40 (m, 3H), 7.40–7.33 (m, 1H), 6.91 (dd, J = 7.6, 1.0 Hz, 1H), 4.27 (m, 1H), 4.21–4.09 (m, 2H), 3.69 (t, J = 6.0 Hz, 2H), 2.74–2.52 (m, 14H); ^{13}C NMR (126 MHz, Methanol-d_4) δ 155.87, 136.04, 128.45, 127.37, 126.99, 126.07, 123.02, 121.41, 105.98, 72.13, 68.45, 62.36, 61.25, 59.77, 54.43, 54.35; HRMS: m/z 331.20111 [M+H]+ (calculated m/z 331.20162 for [C19H27N2O3]+).

*4.2.1.2. 1-(4-(2-hydroxyethyl)piperazin-1-yl)-3-(naphthalen-2-yloxy)propan-2-ol (**3b**).* Yellow oil (0,42 g, 85%); ^{1}H NMR (500 MHz, Methanol-d_4) δ 7.78–7.71 (m, 3H), 7.45–7.38 (m, 1H), 7.34–7.28 (m, 1H), 7.24 (d, J = 2.5 Hz, 1H), 7.18 (dd, J = 9.0, 2.5 Hz, 1H), 4.22–4.15 (m, 1H), 4.12 (dd, J = 9.8, 4.1 Hz, 1H), 4.05 (dd, J = 9.8, 5.9 Hz, 1H), 3.69 (t, J = 5.9 Hz, 2H), 2.75–2.47 (m, 12H); ^{13}C NMR (126 MHz, Methanol-d_4) δ 158.21, 136.10, 130.54, 130.36, 128.57, 127.82, 127.33, 124.65, 119.80, 107.78, 71.96, 68.33, 62.17, 61.25, 59.77, 54.41, 54.33; HRMS: m/z 331.20102 [M+H]+ (calculated m/z 331.20162 for [C19H27N2O3]+).

*4.2.1.3. 1-(4-(2-hydroxyethyl)piperazin-1-yl)-3-(4-methylphenoxy) propan-2-ol (**3c**).* White solid, m. p. 201–203 °C (0,30 g, 69%); ^{1}H NMR (500 MHz, Methanol-d_4) δ 7.11–7.03 (m, 2H), 6.89–6.78 (m, 2H), 4.14–4.05 (m, 1H), 3.95 (dd, J = 9.8, 4.3 Hz, 1H), 3.89 (dd, J = 9.8, 5.9 Hz, 1H), 3.69 (t, J = 5.9 Hz, 2H), 2.70–2.46 (m, 12H), 2.26 (s, 3H); ^{13}C NMR (126 MHz, Methanol-d_4) δ 158.22, 131.12, 130.82, 115.46, 71.98, 68.38, 62.18, 61.25, 59.78, 54.40, 54.32, 20.52; HRMS: m/z 295.20117 [M+H]+ (calculated m/z 295.20162 for [C16H27N2O3]+).

*4.2.1.4. 1-(4-(2-hydroxyethyl)piperazin-1-yl)-3-phenoxypropan-2-ol (**3d**).* Yellow oil (0,28 g, 67%); ^{1}H NMR (500 MHz, DMSO-d_6) δ 7.31–7.22 (m, 3H), 6.94–6.90 (m, 2H), 6.67 (m, 1H), 3.98–3.89 (m, 2H), 3.87–3.79 (m, 1H), 3.46 (t, J = 6.4 Hz, 2H), 2.48–2.28 (m, 12H); ^{13}C NMR (126 MHz, DMSO-d_6) δ 158.90, 129.62, 120.59, 114.65, 71.13, 66.66, 61.28, 58.67, 53.71, 53.47, 22.68; HRMS: m/z 281.18527 [M+H]+ (calculated m/z 281.18597 for [C15H25N2O3]+).

*4.2.1.5. 1-(4-(2-hydroxyethyl)piperazin-1-yl)-3-(2-methoxy-4-nitrophenoxy)propan-2-ol (**3e**).* Yellow solid, m. p. 184–186 °C (0,47 g, 88%);^{1}H NMR (500 MHz, DMSO-d_6) δ 7.87 (dd, J = 9.0, 2.7 Hz, 1H), 7.73 (d, J = 2.7 Hz, 1H), 7.19 (d, J = 9.0 Hz, 1H), 4.12 (dd, J = 9.8, 3.0 Hz, 1H), 4.05–3.94 (m, 2H), 3.88 (s, 3H), 3.46 (t, J = 6.3 Hz, 2H), 2.48–2.31 (m, 12H); ^{13}C NMR (126 MHz, DMSO-d_6) δ 154.44, 148.90, 140.75, 117.82, 112.01, 106.72, 72.61, 66.46, 61.14, 58.66, 56.20, 53.69, 53.45, 22.68; HRMS: m/z 356.18094 [M+H]+ (calculated m/z 356.18161 for [C16H26N3O6]+).

*4.2.1.6. 1-(4-(2-hydroxyethyl)piperazin-1-yl)-3-(2-isopropyl-5-methylphenoxy)propan-2-ol (**3f**).* Yellow oil (0,36 g, 71%); ^{1}H NMR (500 MHz, DMSO-d_6) δ 7.02 (d, J = 7.6 Hz, 1H), 6.72 (d, J = 1.5 Hz, 1H), 6.68 (dd, J = 7.6, 1.5 Hz, 1H), 3.97–3.88 (m, 2H), 3.88–3.81 (m, 1H), 3.46 (t, J = 6.3 Hz, 2H), 3.27–3.17 (m, 1H), 2.52–2.31 (m, 12H),

2.24 (s, 3H), 1.13 (dd, $J = 6.9$, 1.3 Hz, 6H); ^{13}C NMR (126 MHz, DMSO-d_6) δ 155.82, 135.95, 133.36, 125.68, 121.02, 112.60, 70.97, 66.74, 61.44, 60.50, 58.67, 53.78, 53.47, 26.23, 22.85, 22.83, 21.13; HRMS: *m/z* 337.24792 [M+H]+ (calculated *m/z* 337.24857 for [C19H33N2O3]+).

*4.2.1.7. 1-(2,6-dimethoxyphenoxy)-3-(4-(2-hydroxyethyl)piperazin-1-yl)propan-2-ol (**3g**).* Yellow oil (0,41 g, 81%);^{1}H NMR (500 MHz, Methanol-d_4) δ 7.02 (t, $J = 8.4$ Hz, 1H), 6.67 (d, $J = 8.4$ Hz, 2H), 4.08−3.99 (m, 1H), 3.95 (dd, $J = 10.1$, 4.9 Hz, 1H), 3.86 (dd, $J = 10.1$, 6.2 Hz, 1H), 3.84 (s, 6H), 3.69 (t, $J = 6.0$ Hz, 2H), 2.70−2.60 (m, 10H), 2.55 (t, $J = 6.0$ Hz, 2H), 2.51 (dd, $J = 13.1$, 7.9 Hz, 1H); ^{13}C NMR (126 MHz, Methanol-d_4) δ 154.70, 138.39, 125.16, 106.63, 77.24, 68.94, 62.01, 61.24, 59.76, 56.57, 54.36, 54.23; HRMS: *m/z* 341.20691 [M+H]+ (calculated *m/z* 341.20710 for [C17H29N2O5]+).

*4.2.1.8. 1-(4-Allyl-2-methoxyphenoxy)-3-(4-(2-hydroxyethyl)piperazin-1-yl)propan-2-ol (**3h**).* Yellow oil (0,42 g, 79%); ^{1}H NMR (500 MHz, Methanol-d_4) δ 6.89 (d, $J = 8.1$ Hz, 1H), 6.81 (d, $J = 2.1$ Hz, 1H), 6.72 (dd, $J = 8.2$, 2.0 Hz, 1H), 6.02−5.90 (m, 1H), 5.10−5.00 (m, 2H), 4.17−4.08 (m, 1H), 3.98 (dd, $J = 9.9$, 4.4 Hz, 1H), 3.91 (dd, $J = 9.9$, 6.0 Hz, 1H), 3.83 (s, 3H), 3.70 (t, $J = 6.0$ Hz, 2H), 3.33 (d, $J = 1.5$ Hz, 1H), 2.74−2.54 (m, 13H); ^{13}C NMR (126 MHz, Methanol-d_4) δ 150.87, 148.05, 139.12, 135.06, 121.96, 115.75, 115.54, 113.96, 73.61, 68.38, 61.87, 61.05, 59.46, 56.49, 54.10, 54.08, 40.73; HRMS: *m/z* 351.22748 [M+H]+ (calculated *m/z* 351.22783 for [C19H31N2O4]+).

*4.2.1.9. 1-(4-(2-hydroxyethyl)piperazin-1-yl)-3-(2-methoxyphenoxy) propan-2-ol (**3i**).* White solid, m. p. 192−194 °C (0,34 g, 74%); ^{1}H NMR (500 MHz, Methanol-d_4) δ 7.01−6.88 (m, 4H), 4.18 (m, 1H), 4.01 (dd, $J = 9.8$, 4.5 Hz, 1H), 3.96 (dd, $J = 9.8$, 5.8 Hz, 1H), 3.85 (d, $J = 5.0$ Hz, 3H), 3.76 (t, $J = 5.6$ Hz, 2H), 3.03−2.67 (m, 10H), 1.94 (d, $J = 0.6$ Hz, 3H); ^{13}C NMR (126 MHz, Methanol-d_4) δ 150.96, 149.67, 122.91, 122.26, 115.42, 113.49, 73.18, 68.06, 61.33, 60.43, 58.52, 56.49, 53.43, 53.22, 22.08; HRMS: *m/z* 311.19586 [M+H]+ (calculated *m/z* 311.19653 for [C16H27N2O4]+).

*4.2.1.10. 1-(4-(2-hydroxyethyl)piperazin-1-yl)-3-(2-methylphenoxy) propan-2-ol (**3j**).* Yellow oil (0,30 g, 67%); ^{1}H NMR (500 MHz, Methanol-d_4) δ 7.17−7.09 (m, 2H), 6.89 (dd, $J = 8.1$, 1.0 Hz, 1H), 6.87−6.81 (m, 1H), 4.23 (s, 1H), 4.01 (d, $J = 5.0$ Hz, 2H), 3.87−3.81 (m, 2H), 3.23−3.19 (m, 8H), 3.12−3.09 (m, 3H), 2.93−2.89 (m, 3H), 2.23 (s, 3H); ^{13}C NMR (126 MHz, Methanol-d_4) δ 158.15, 131.61, 127.95, 127.75, 121.80, 112.32, 71.40, 60.92, 59.67, 52.78, 49.51, 49.34, 49.17, 49.00, 48.83, 48.66, 48.49, 22.08, 16.37; HRMS: *m/z* 295.20099 [M+H]+ (calculated *m/z* 295.20162 for [C16H27N2O3]+).

4.3. In vitro cytotoxicity

4.3.1. Cell cultivation and treatment

The selected 10 human cell lines − Jurkat (acute T-cell leukemia), MOLT-4 (acute lymphoblastic leukemia), A2780 (ovarian carcinoma), A549 (lung carcinoma), HT-29 (colorectal adenocarcinoma), PANC-1 (pancreas epithelioid carcinoma), HeLa (cervix adenocarcinoma), MCF-7 (breast adenocarcinoma), SAOS-2 (osteosarcoma), and MRC-5 (lung fibroblast) − were purchased from Sigma Aldrich and cultivated according to the provider's culture method guidelines. At the start of experiments, each cell line was seeded at previously established optimal density (500−30 $\times$ 10^3 cells per well) in a 96-well plate and the cells were allowed to settle overnight. The derivatives to be tested were dissolved in DMSO to stock solutions (10 mM). For the experiments, the stock solution was diluted with the appropriate complete culture medium to reach final concentrations of 10 and 100 μM. Cells were exposed to 10 and 100 μM newly synthesized inhibitors for 48 h. Cells were also exposed to doxorubicin at a concentration of 1 μM. The maximal concentration of DMSO in cultivation media was 0.1%.

4.3.2. Cell proliferation assay and growth percent calculation

The WST-1 (Roche, Mannheim, Germany) reagent was used to determine the cytotoxic effect of the tested compounds. At the end of the cultivation period, WST-1 test was performed according to the manufacturer's protocol. The absorbance was measured using a Tecan Infinite M200 spectrometer (Tecan Group, Männedorf, Switzerland). Each value is the mean of three independent experiments and represents the percentage of proliferation of control, non-treated cells (100%). The GP value was calculated for each inhibitor tested. GP represents the mean of viability decrease as a percentage of all the 10 cell lines treated with the same inhibitor.

4.4. Half maximal inhibitory concentration (IC_{50}) and maximum tolerated concentration (MTC)

For the cytotoxicity assays, A-549 cells were cultivated in Dulbecco's modified Eagle's medium (DMEM, Biosera, Nuaille, France) supplemented with 10% fetal bovine serum (Biosera) and 1% penicillin-streptomycin antibiotic solution (Sigma−Aldrich). The cells were maintained in a humidified atmosphere of 5% CO_2 at 37 °C.

Cell viability was evaluated by colorimetric viability assay according to Muckova et al. (2018). Briefly, A-549 cells were plated into 96-well plates in a volume of 100 μL and density of 9 $\times$ 10^3 cells per well. Cells were left to attach overnight. The working solutions of tested compounds were prepared in phosphate buffer saline (PBS; Sigma−Aldrich) and serially diluted in DMEM. For determination of 100% viability, we measured the untreated control in each plate. After 24 h incubation, the cell viability was determined using colorimetric MTT (3-(4,5-dimethylthiazol-2-yl)-2,5-diphenyltetrazolium bromide (Sigma−Aldrich) reduction assay. The experiment was carried out in triplicate and repeated three independent times.

4.4.1. Statistical analysis

The IC_{50} values were calculated using four parametric nonlinear regressions by GraphPad Prism statistics software (version 5.04, GraphPad Software Inc., San Diego, CA, USA) from the logarithmic concentration-response curve. The values were expressed as a mean ± standard error of the mean (SEM).

4.5. In vitro radioprotection studies

4.5.1. Cell treatment and gamma irradiation

Fresh stock solutions of PUMA inhibitors in concentrations of 50 mM were dissolved in dimethyl sulfoxide - DMSO (Sigma-Aldrich, St. Louis, MO, USA). Stock solutions were freshly prepared before use in the study. For the radioprotection experiments, MOLT-4 cells were treated with inhibitors at 100 μM, making sure the concentration of DMSO was <0.1% to avoid toxic effects on the cells. Sixty minutes after inhibitor addition, MOLT-4 cells were irradiated at room temperature using a ^{60}Co γ-ray source (Chisotron Chirana, Prague, Czech Republic). Non-irradiated control and irradiated-alone cells were treated with a DMSO vehicle only (0.1%; Control) and handled in parallel with the test cells. Non-irradiated control cells were handled in the same way as described for inhibitor-treated cells, except that irradiation was omitted.

4.5.2. Analysis of viability

Viability was determined by flow cytometry using an Alexa Fluor® 488 Annexin V/Dead Cell Apoptosis kit (Life Technologies, Grand Island, NY, USA) according to the manufacturer's instructions. The Alexa Fluor® 488 Annexin V/Dead Cell Apoptosis kit employs the property of Alexa Fluor® 488 conjugated to Annexin V to bind to phosphatidylserine in the presence of Ca^{2+}, and the property of PI to enter cells with damaged cell membranes and to bind to DNA. Measurement was performed immediately using a CyAn (Beckman Coulter, Miami, FL, USA) flow cytometer. Listmode data were analysed using Kaluza Analysis 1.3 software (Beckman Coulter, Miami, FL, USA).

4.5.3. Statistical analysis

The descriptive statistics of the results were calculated, and the charts made in either Microsoft Office Excel 2010 (Microsoft, Redmond, WA, USA) or GraphPad Prism 5 biostatistics (GraphPad Software, La Jolla, CA, USA). In this study, all of the values were expressed as arithmetic means with SD of triplicates, unless otherwise noted. The significant differences between the groups were analyzed using the Student's t-test and a P value < 0.05 was considered significant.

4.6. Protective effect on mice

4.6.1. Animals and irradiation

Experimental C57Bl/6 mice (27 ± 3 g) were obtained from Velaz a.s. (Prague, Czech Republic). All used methods were in accordance to EU Directive 2010/63/EU for animal experiments and NIRS Guidelines for the Care and Use of Laboratory Animals and approved by the Committee for animal rights of the Ministry of Defence of Czech Republic. The mice were organized in groups of 10 animals each and received a dose of 8.5 G from a ^{60}Co gamma source (Chisotron, Chirana, Czech Republic) at a dose rate of 1.3 Gy/min; non-irradiated and non-treated control groups were also included. Their survival and health status was monitored on a daily basis for 30 days.

4.6.2. Radioprotective compounds

Selected compounds, identified by numbers: **3e**, **3g**, **3h**, **3i** and **3j**, were prepared before each experiment from a 100 mg/ml stock solution to a working concentration of 100 mg/kg applied i.p. 5 min before irradiation.

4.6.3. Blood collection

Peripheral blood was collected on days 0, 7, 12 and 30 of the experiments. The blood, taken by cardiac puncture after inhalation anaesthesia of each mouse by exposure to increasing concentrations of CO_2, was collected in a 1.0 mL BD Microtainer MAP K_2EDTA (Becton Dickinson, Sarstedt Ltd, Leicester, United Kingdom) and used for the determination of absolute cell count and lymphocyte population analysis.

4.6.4. Analysis of absolute blood counts

100 μl of blood was used for analysis of the complete blood counts using an automated hematological analyser Pentra 60 ABX (Horiba, Japan).

4.6.5. Flow cytometry analysis of T and B lymphocytes and NK cells in the peripheral blood

A mixture of monoclonal antibodies (1 μl of CD3ε V500, 1 μl of CD19 APC and 1 μl NK1.1 PEcy7, all from BD Biosciences) and 100 μl of peripheral blood was cultivated (30 min, 4 °C, dark). The cell suspension was then washed twice (5 ml of CellWash added, and centrifuged for 10 min at 4 °C), and samples were measured by flow cytometer CyAn ADP (Beckman Coulter, San Jose, CA, US).

Author contributions

The manuscript was written through contributions of all authors. All authors have given approval to thefinal version of themanuscript.

Declarations of interest

None.

Acknowledgements

This work was supported by grant project No. 17-13541S of the Czech Science Foundation.

Appendix A. Supplementary data

Supplementary data to this article can be found online at https://doi.org/10.1016/j.ejmech.2019.111606.

References

[1] R. Yahyapour, P. Amini, S. Rezapour, M. Cheki, A. Rezaeyan, B. Farhood, D. Shabeeb, A.E. Musa, H. Fallah, M. Najafi, Radiation-induced inflammation and autoimmune diseases, Mil. Med. Res. 5 (2018). https://doi.org/10.1186/s40779-018-0156-7.

[2] M. Sadeghi, M. Enferadi, A. Shirazi, External and internal radiation therapy: past and future directions, J. Cancer Res. Ther. 6 (3) (2010) 239–248. https://doi.org/10.4103/0973-1482.73324.

[3] M. Najafi, E. Motevaseli, A. Shirazi, G. Geraily, A. Rezaeyan, F. Norouzi, S. Rezapoor, H. Abdollahi, Mechanisms of inflammatory responses to radiation and normal tissues toxicity: clinical implications, Int. J. Radiat. Biol. 94 (4) (2018) 335–356. https://doi.org/10.1080/09553002.2018.1440092.

[4] K. Mortezaee, N.H. Goradel, P. Amini, D. Shabeeb, A.E. Musa, M. Najafi, B. Farhood, NADPH oxidase as a target for modulation of radiation response; implications to carcinogenesis and radiotherapy, Curr. Mol. Pharmacol. 12 (1) (2019) 50–60. https://doi.org/10.2174/1874467211666181010154709.

[5] K.N. Mishra, B.A. Moftah, G.A. Alsbeih, Appraisal of mechanisms of radioprotection and therapeutic approaches of radiation countermeasures, Biomed. Pharmacother. Biomedecine Pharmacother. 106 (2018) 610–617. https://doi.org/10.1016/j.biopha.2018.06.150.

[6] M. Hassan, H. Watari, A. AbuAlmaaty, Y. Ohba, N. Sakuragi, Apoptosis and molecular targeting therapy in cancer, BioMed Res. Int. 2014 (2014). https://doi.org/10.1155/2014/150845.

[7] A. Tichy, J. Marek, R. Havelek, J. Pejchal, M. Seifrtova, L. Zarybnicka, A. Filipova, M. Rezacova, Z. Sinkorova, New light on an old friend: targeting PUMA in radioprotection and therapy of cardiovascular and neurodegenerative diseases, Curr. Drug Targets 19 (16) (2018) 1943–1957. https://doi.org/10.2174/1389450119666180406110743.

[8] B.J. Leibowitz, W. Qiu, H. Liu, T. Cheng, L. Zhang, J. Yu, Uncoupling P53 functions in radiation-induced intestinal damage via PUMA and P21, Mol. Cancer Res. MCR 9 (5) (2011) 616–625. https://doi.org/10.1158/1541-7786.MCR-11-0052.

[9] L. Ming, T. Sakaida, W. Yue, A. Jha, L. Zhang, J. Yu, Sp1 and P73 activate PUMA following serum starvation, Carcinogenesis 29 (10) (2008) 1878–1884. https://doi.org/10.1093/carcin/bgn150.

[10] R.M. Ray, S. Bhattacharya, L.R. Johnson, Mdm2 inhibition induces apoptosis in P53 deficient human colon cancer cells by activating P73- and E2F1-mediated expression of PUMA and siva-1, Apoptosis Int. J. Program. Cell Death 16 (1) (2011) 35–44. https://doi.org/10.1007/s10495-010-0538-0.

[11] Q. Sun, L. Ming, S.M. Thomas, Y. Wang, Z.G. Chen, R.L. Ferris, J.R. Grandis, L. Zhang, J. Yu, PUMA mediates EGFR tyrosine kinase inhibitor-induced apoptosis in head and neck cancer cells, Oncogene 28 (24) (2009) 2348–2357. https://doi.org/10.1038/onc.2009.108.

[12] P. Wang, W. Qiu, C. Dudgeon, H. Liu, C. Huang, G.P. Zambetti, J. Yu, L. Zhang, PUMA is directly activated by NF-KappaB and contributes to TNF-alpha-induced apoptosis, Cell Death Differ. 16 (9) (2009) 1192–1202. https://doi.org/10.1038/cdd.2009.51.

[13] G. Mustata, M. Li, N. Zevola, A. Bakan, L. Zhang, M. Epperly, J.S. Greenberger, J. Yu, I. Bahar, Development of small-molecule PUMA inhibitors for mitigating radiation-induced cell death, Curr. Top. Med. Chem. 11 (3) (2011) 281–290. https://doi.org/10.2174/156802611794072641.

[14] Procedimiento De Obtencion De 1-Ariloxi - 2 - Propanolami- Nas Farmacologicamente Activos. ES411826, 1976 (A1), January 1.

[15] ZINC22465724, ZINC Is Not Commercial - a database of commercially-

available compounds. https://zinc.docking.org/substance/22465724. (Accessed 19 June 2019).
[16] ZINC19790808, ZINC Is Not Commercial - a database of commercially-available compounds. https://zinc.docking.org/substance/19790808. (Accessed 19 June 2019).
[17] ZINC19882186, ZINC Is Not Commercial - a database of commercially-available compounds. https://zinc.docking.org/substance/19882186. (Accessed 19 June 2019).
[18] ZINC20707440, ZINC Is Not Commercial - a database of commercially-available compounds. https://zinc.docking.org/substance/20707440. (Accessed 19 June 2019).
[19] H. Marona, M. Kubacka, B. Filipek, A. Siwek, M. Dybaia, E. Szneler, T. Pociecha, A. Gunia, A.M. Waszkielewicz, Synthesis, alpha-adrenoceptors affinity and alpha(1)-adrenoceptor antagonistic properties of some 1,4-substituted piperazine derivatives, Die Pharmazie 66 (10) (2011) 733–739. https://doi.org/10.1691/ph.2011.1543.
[20] W.E. Kreighbaum, W.L. Matier, R.D. Dennis, J.L. Minielli, D. Deitchman, J.L. Perhach, W.T. Comer, Antihypertensive indole derivatives of phenoxypropanolamines with .Beta.-Adrenergic receptor antagonist and vasodilating activity, J. Med. Chem. 23 (3) (1980) 285–289. https://doi.org/10.1021/jm00177a015.
[21] L. Stankyavichene, A. Stankyavichus, M. Sapragonene, S. Risyalis, P. Terentjev, K. Azhami, G. Vladyko, L. Korobchenko, E. Borenko, Synthesis of 2-(1-aryloxy-2-oxypropylamino) and 2-(1-arylamino-2-oxypropylamino)pyrimidines and their acyclic analogs and study of their antiviral activity, Khim. Farm. Zh. 21 (4) (1987) 459–464.
[22] G.H. Chen, S. Wang, F.H. Wu, A practical synthesis of sarpogrelate hydrochloride and in vitro platelet aggregation inhibitory activities of its analogues, Chin. Chem. Lett. 21 (3) (2010) 287–289. https://doi.org/10.1016/j.cclet.2009.11.030.
[23] A.J. Souers, J.D. Leverson, E.R. Boghaert, S.L. Ackler, N.D. Catron, J. Chen, B.D. Dayton, H. Ding, S.H. Enschede, W.J. Fairbrother, et al., ABT-199, a potent and selective BCL-2 inhibitor, achieves antitumor activity while sparing platelets, Nat. Med. 19 (2) (2013) 202–208. https://doi.org/10.1038/nm.3048.
[24] J. Marek, D. Malinak, R. Dolezal, O. Soukup, M. Pasdiorova, M. Dolezal, K. Kuca, Synthesis and disinfection effect of the pyridine-4-aldoxime based salts, Molecules 20 (3) (2015) 3681–3696. https://doi.org/10.3390/molecules20033681.
[25] J. Garrett, C.M. Orschell, M.S. Mendonca, R.M. Bigsby, J.R. Dynlacht, Subcutaneous wounding postirradiation reduces radiation lethality in mice, Radiat. Res. 181 (6) (2014) 578–583. https://doi.org/10.1667/RR13267.1.
[26] R. van Os, C. Lamont, A. Witsell, P.M. Mauch, Radioprotection of bone marrow stem cell subsets by interleukin-1 and kit-ligand: implications for CFU-S as the responsible target cell population, Exp. Hematol. 25 (3) (1997) 205–210.
[27] P.A. Plett, H.L. Chua, C.H. Sampson, B.P. Katz, C.M. Fam, L.J. Anderson, G.N. Cox, C.M. Orschell, PEGylated G-CSF (BBT-015), GM-CSF (BBT-007), and IL-11 (BBT-059) analogs enhance survival and hematopoietic cell recovery in a mouse model of the hematopoietic syndrome of the acute radiation syndrome, Health Phys. 106 (1) (2014) 7–20. https://doi.org/10.1097/HP.0b013e3182a4dd4e.
[28] I. Vogler, I. Kneiske, A. Muik, D. von Laer, Lcmv-pseudotyped vsv-vectors for treatment of malignant glioma, Neuro Oncol. 11 (5) (2009), 594–594.
[29] N.S. Kalman, S.S. Zhao, M.S. Anscher, A.I. Urdaneta, Current status of targeted radioprotection and radiation injury mitigation and treatment agents: a critical review of the literature, Int. J. Radiat. Oncol. Biol. Phys. 98 (3) (2017) 662–682. https://doi.org/10.1016/j.ijrobp.2017.02.211.
[30] K. Mortezaee, D. Shabeeb, A.E. Musa, M. Najafi, B. Farhood, Metformin as a radiation modifier; implications to normal tissue protection and tumor sensitization, Curr. Clin. Pharmacol. 14 (1) (2019) 41–53. https://doi.org/10.2174/1574884713666181025141559.
[31] U. Weyemi, C.E. Redon, T. Aziz, R. Choudhuri, D. Maeda, P.R. Parekh, M.Y. Bonner, J.L. Arbiser, W.M. Bonner, Inactivation of NADPH oxidases NOX4 and NOX5 protects human primary fibroblasts from ionizing radiation-induced DNA damage, Radiat. Res. 183 (3) (2015) 262–270. https://doi.org/10.1667/RR13799.1.
[32] Y. Wang, Q. Liu, W. Zhao, X. Zhou, G. Miao, C. Sun, H. Zhang, NADPH oxidase activation contributes to heavy ion irradiation-induced cell death, Dose-Response Publ. Int. Hormesis Soc. 15 (1) (2017), 1559325817699697, https://doi.org/10.1177/1559325817699697.
[33] K.L. Burr, J.I. Robinson, S. Rastogi, M.T. Boylan, P.J. Coates, S.A. Lorimore, E.G. Wright, Radiation-induced delayed bystander-type effects mediated by hemopoietic cells, Radiat. Res. 173 (6) (2010) 760–768. https://doi.org/10.1667/RR1937.1.
[34] G. Ramachandran, C. Ramakrishnan, V. Sasisekharan, Stereochemistry of polypeptide chain configurations, J. Mol. Biol. 7 (1963) 95–99. https://doi.org/10.1016/S0022-2836(63)80023-6.
[35] UCSF Chimera—A Visualization System for Exploratory Research and Analysis - Pettersen - 2004 - Journal of Computational Chemistry, Wiley Online Library, 2004. https://onlinelibrary.wiley.com/doi/abs/10.1002/jcc. (Accessed 19 June 2019).
[36] G.M. Morris, R. Huey, W. Lindstrom, M.F. Sanner, R.K. Belew, D.S. Goodsell, A.J. Olson, AutoDock4 and AutoDockTools4: automated docking with selective receptor flexibility, J. Comput. Chem. 30 (16) (2009) 2785–2791. https://doi.org/10.1002/jcc.21256.
[37] N.M. O'Boyle, M. Banck, C.A. James, C. Morley, T. Vandermeersch, G.R. Hutchison, Open Babel: an open chemical toolbox, J. Cheminf. 3 (2011) 33. https://doi.org/10.1186/1758-2946-3-33.
[38] M.D. Hanwell, D.E. Curtis, D.C. Lonie, T. Vandermeersch, E. Zurek, G.R. Hutchison, Avogadro: an advanced semantic chemical editor, visualization, and analysis platform, J. Cheminf. 4 (1) (2012) 17. https://doi.org/10.1186/1758-2946-4-17.
[39] O. Trott, A.J. Olson, AutoDock Vina: improving the speed and accuracy of docking with a new scoring function, efficient optimization, and multithreading, J. Comput. Chem. 31 (2) (2010) 455–461. https://doi.org/10.1002/jcc.21334.

Please cite this article as: J. Marek et al., A novel class of small molecule inhibitors with radioprotective properties, European Journal of Medicinal Chemistry, https://doi.org/10.1016/j.ejmech.2019.111606